JTTEE5 9:499-504

Properties of Cr_3C_2-NiCr Cermet Coating Sprayed by High Power Plasma and High Velocity Oxy-Fuel Processes

F. Otsubo, H. Era, T. Uchida, and K. Kishitake

(Submitted 28 February 2000)

The structure, hardness, and shear adhesion strength have been investigated for Cr_3C_2-NiCr cermet coatings sprayed onto a mild steel substrate by 200 kW high power plasma spraying (HPS) and high velocity oxy-fuel (HVOF) processes. Amorphous and supersaturated nickel phases form in both as-sprayed coatings. The hardness of the HVOF coating is higher than that of the HPS coating, because the HVOF coating contains more nonmelted Cr_3C_2 carbide particles. On heat treating at 873 K, the amorphous phase decomposes and the supersaturated nickel phase precipitates Cr_3C_2 carbides so that the hardness increases in the HPS coating.

The hardness measured under a great load exhibits lower values compared with that measured with a small load because of cracks generated from the indentation. The ratio of the hardnesses measured with different loads can be regarded as an index indicating the coating ductility. The ductility of the HVOF coating is higher than that of the HPS coating. Adhesion strength of the HVOF coating was high compared with the HPS coating. The adhesion of the coatings is enhanced by heat treating at 1073 K, and that of the HVOF coating is over 350 MPa.

Keywords adhesion strength, Cr_3C_2 cermet coating, ductility, high power plasma spraying, high velocity oxy-fuel

1. Introduction

Chromium carbide, Cr_3C_2 with NiCr, coatings exhibit heat resistance and wear resistance and are applied for heat-treatment rolls[1,2] and coal burning boiler tubes, because of their superior heat resistance and erosion resistance against fly ash.[3] It is also expected in the future that such cermet coatings will be used for structural parts in high-temperature environments.

High-quality coatings have been obtained through the extensive development of a thermal spraying apparatus, such as high velocity flame spraying (high velocity oxy-fuel (HVOF) and high velocity air-fuel (HVAF) and high power plasma spraying (HPS). In the former process, the decomposition of the spray material is retarded due to the high flame speed and the low flame temperature. In the latter process, although materials of high melting point can be sprayed and a dense coating is obtained, this process has a disadvantage due to decomposition of hard materials[4] because of the high temperature.

It is known that the properties of cermet coatings markedly depend on the structure of the coatings.[5,6] Though there are some investigations concerning the properties of Cr_3C_2 cermet coating,[3,6–9] most of them do not evaluate the characteristics of coatings, but measure only a property of the coating, such as wear resistance. The aim of this work is to characterize the structure and properties of Cr_3C_2 cermet coatings thermal sprayed by HVOF and HPS processes.

2. Experimental Procedure

The cermet powder (75 mass% Cr_3C_2-25 mass% NiCr, SHOWA DENKO SHOCOAT KC-21E; Showa Denko, Minato, Tokyo, Japan, +16–53 μm particle size range) used in this study was manufactured by sintering. Figure 1 shows an scanning electron microscopy (SEM) image of the powder used. The powder was thermal sprayed onto a mild steel substrate (JIS-SS400) using 200 kW HPS and HVOF processes. The coating thickness was about 350 μm. The spraying conditions of the HPS (PLAZ-JET III-250) and HVOF (HOBART TAFA JP-5000 HP/HVOF Spray System) processes are shown in Tables 1 and 2, respectively.

The structure and phases in the as-sprayed and heat-treated coatings were examined by means of electron probe microanalysis (EPMA) and x-ray diffraction (XRD) with Cu $K\alpha$ radiation. The heat treatment was carried out in vacuum at temperatures up to 1273 K for 3.6 ks. The hardness of the coatings was measured at more than 15 randomly located positions on the cross section for each specimen by a Vickers microhardness tester, and adhesion strength of the coating was evaluated for 10 specimens at each spray condition by a shear test. Shear test pieces used in this study have a semicircular notch of 0.4 mm in radius, proposed by the authors, as shown in Fig. 2, to reduce the stress concentration at the corner of the protruded step.[10]

F. Otsubo, H. Era, and **K. Kishitake,** Department of Materials Science and Engineering, Faculty of Engineering, Kyushu Institute of Technology, Kita-Kyushu 804-8550, Japan; and **T. Uchida,** Department of Materials Science and Engineering, Kyushu Institute of Technology. Contact e-mail: otsubo@tobata.isc.kyutech.ac.jp.

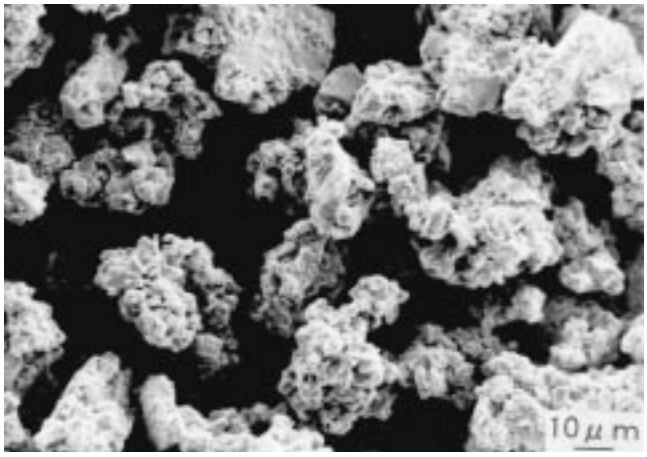

Fig. 1 SEM image of powder for spraying

Table 1 Plasma spraying processing parameters

Current	500 A
Voltage	423 V
Plasma gas	150 (Ar) and 330 (N_2) L/min
Feed rate	20 kg/h
Spray distance	200 mm

Table 2 HVOF spray processing parameters

Kerosine	18.9 L/h
Oxygen	5×10^4 L/h
Powder	3.4 kg/h
Spray distance	350 mm

3. Results and Discussion

3.1 Structure and Phases

Figure 3 shows backscattered electron (BSE) images of the as-sprayed coatings by the HPS and HVOF processes. The granular dark particles, as shown by arrows, are Cr_3C_2 carbides, which are deposited without melting. More granular Cr_3C_2 particles remained in the HVOF coating compared with the HPS coating, and the lamellar structure of the HVOF coating is finer than that of the HPS coating. Thus, the spray powders are melted more by the HPS process than the HVOF process because of the temperature difference between the plasma and HVOF flame.

Figure 4 shows the XRD patterns of the original powder and the as-sprayed coatings. Peaks of nickel solid solution and Cr_3C_2 carbide are observed in the pattern of the powder. The XRD patterns of both sprayed coatings are similar. All peaks of nickel solid solution and Cr_3C_2 become broad, and a very broad peak centered around 43° appears in the as-sprayed condition of both coatings. The very broad peak indicates formation of an amorphous phase. Therefore, it is considered that nickel-chromium alloy and some Cr_3C_2 carbide are melted and some amorphous phase forms.

Phase changes of the coatings by heat treatment at various temperatures were investigated by XRD. The XRD patterns of

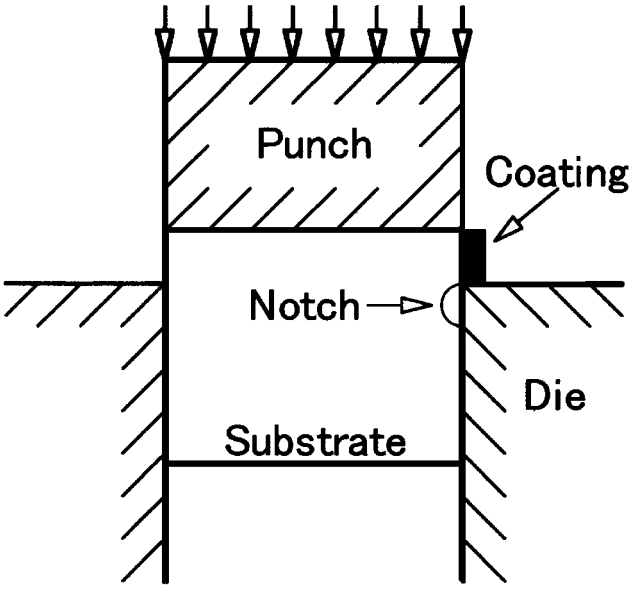

Fig. 2 Schematic illustration of shear test for adhesion strength

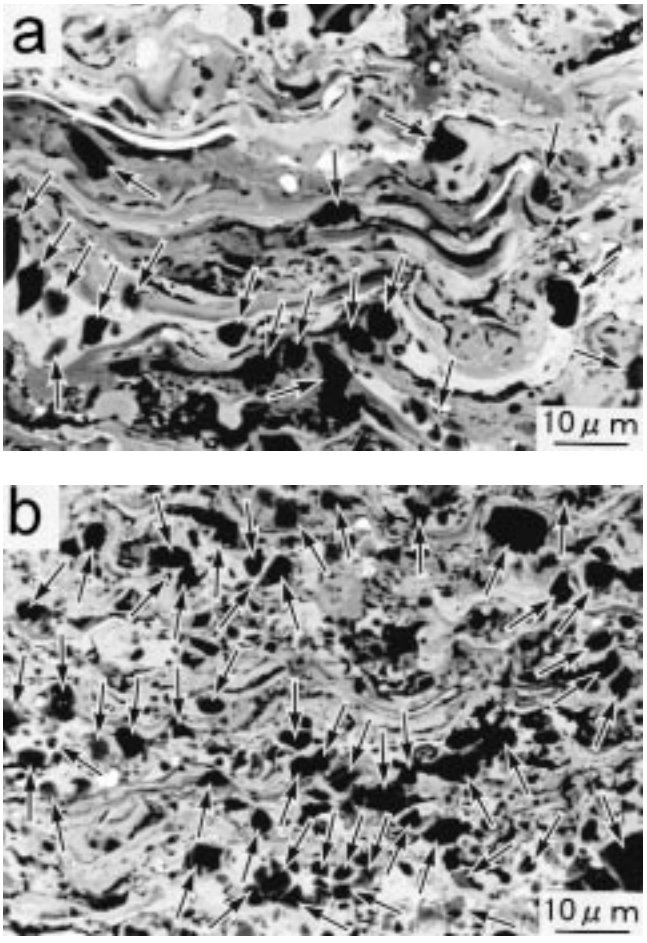

Fig. 3 BSE images of as-sprayed coatings sprayed by (**a**) HPS and (**b**) HVOF processes

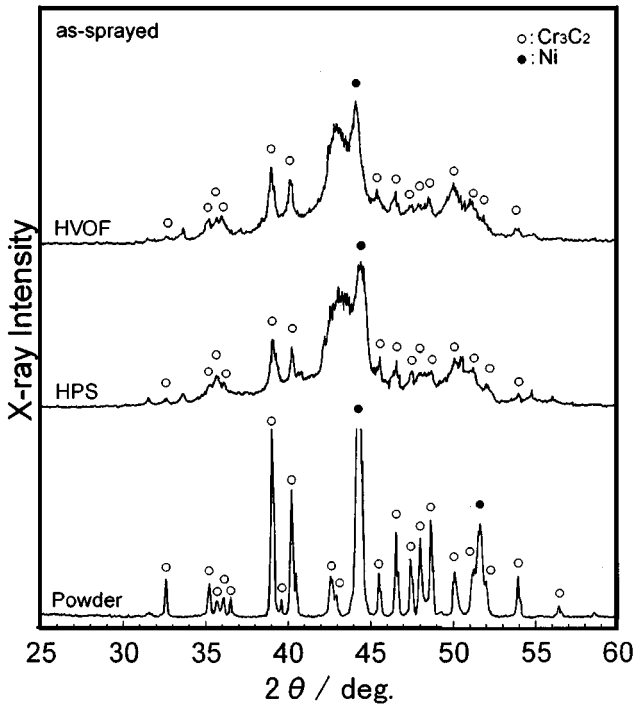

Fig. 4 XRD patterns of powder and as-sprayed coatings

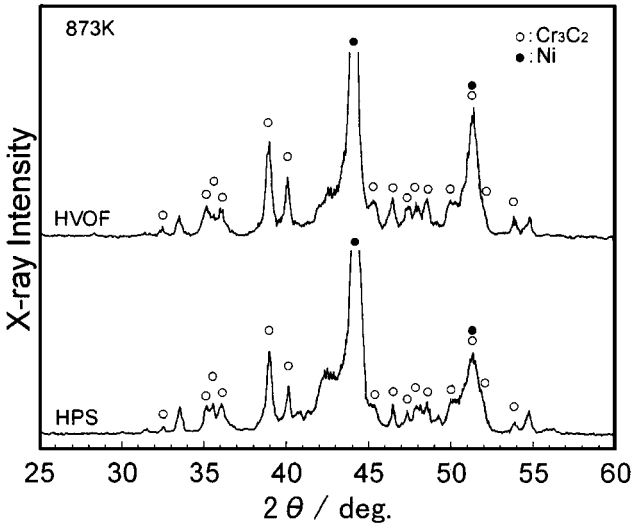

Fig. 5 XRD patterns of coating heat treated at 873 K for 3.6 ks

the coatings heat treated at 673 K were similar to those of the as-sprayed coatings. The very broad peaks of HPS and HVOF disappear on heat treating at 873 K, as shown in Fig. 5, and peaks of nickel solid solution and Cr_3C_2 carbide become sharp compared with those of the as-sprayed coatings. It is seen that the amorphous phase decomposed on heat treating at 873 K. Figure 6 shows XRD patterns of the coatings heat treated at 1073 K. Peaks of nickel solid solution and Cr_3C_2 carbide become clearer.

Figure 7 shows BSE images of the heat-treated HVOF coatings. The coating heat treated at 673 K was similar to the as-

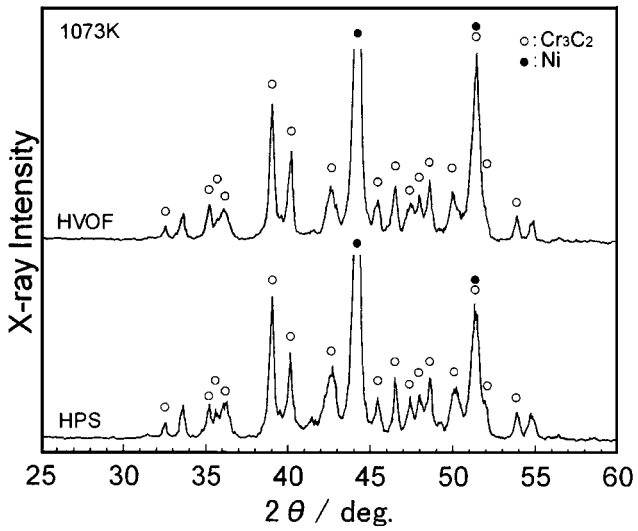

Fig. 6 XRD patterns of coating heat treated at 1073 K for 3.6 ks

sprayed coatings. Fine precipitates in the lamellar structure can be seen in the coatings heat treated at 873 K (Fig.7a). The fine precipitates in the lamellar structure, which are not granular dark particles, as shown in Fig. 3, but are indicated by arrow as the example, grow when heat treated at 1073 and 1273 K (Fig. 7b and c). These fine precipitates are considered from the XRD patterns to be Cr_3C_2 carbides formed by decomposition of the amorphous phase and those precipitated from supersaturated nickel solid solution. The same change in structure of the coating by heat treatment was also seen in HPS coatings.

3.2 Hardness and Adhesion Strength

Figure 8 indicates a change in hardness of the coatings measured with different loads of 9.8 and 49 N as a function of heat-treatment temperature. It is clear that the scatter of hardness is larger and the value of hardness is higher when measured with a low load of 9.8 N compared to the measurement with a high load of 49 N. The hardness of the as-sprayed HVOF coating is higher than that of the HPS coatings at both of these load levels. Therefore, the HVOF coating is denser and contains more retained Cr_3C_2 carbide compared to the HPS coating. The hardness of the HPS coating measured at a load of 9.8 N is enhanced appreciably with the heat-treatment temperature up to 1073 K and nearly attains the hardness of the HVOF coating.

The enhancement of hardness may have resulted from the decomposition of the amorphous phase and the precipitation of Cr_3C_2 carbide in nickel solid solution. The melted proportion is less in the HVOF coating so that the hardness increase is less compared to the HPS coating. The hardness of the HVOF coating increases slightly with the heat-treatment temperature. The hardness of the coatings heat treated at 1273 K decreases due to coarsening of the structure (Fig. 7c). The hardness measured with a load of 49 N is lower than that measured with a load of 9.8 N, and the difference in hardness of the HPS coating is larger than that of the HVOF coating. Lin *et al.* investigated the hardness of the plasma-sprayed materials of metals, intermetallics, and ceramics by different loads on Vickers indentation tests.[11]

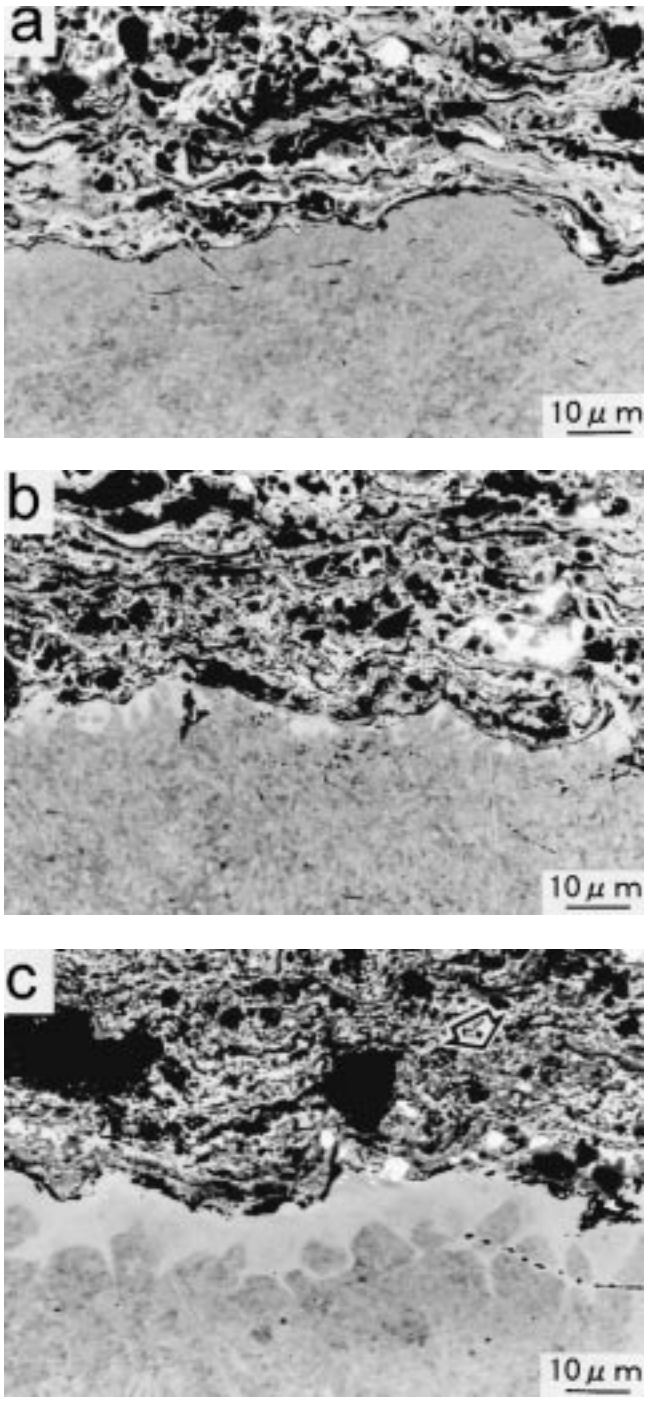

Fig. 7 BSE images of HVOF coatings: (**a**) through (**c**) cross sections of coating with substrate heat treated at 873, 1073, and 1273 K, respectively

They reported that the hardness is enhanced and the data variation becomes large with decreasing load. The tendency is consistent with that formed *via* present work.

Coatings of the HVOF and HPS processes do not exhibit cracks around the hardness indentation when indented with a small load of 9.8 N. The indentation of the HVOF coating also has no visible cracks even when indented with a large load of 49 N. However, cracks developing from an indentation are clearly observed in the HPS coating when indented with a large load of 49 N, as shown by arrows in Fig. 9. Thus, the HPS coatings are more brittle than the HVOF coating.

The difference in the hardness measured with different loads may be the result of cracks that develop from the indentation when measured with a large load and when the hardness is evaluated to be low. Thus, the difference in the hardness becomes more significant when the coating is more brittle. Therefore, the ratio is regarded as an index indicating the ductility of the coating. Figure 10 shows the ratio of the Vickers microhardness measured with a load of 49 N to that measured with a load of 9.8 N as a function of heat-treatment temperature. The ratio of the HVOF coatings is about 0.94 for the as-sprayed and heat-treated coatings. On the other hand, the ratio of the HPS coatings is about 0.84 for the as-sprayed and heat-treated coatings up to 1073 K and increases to 0.87 for the coating heat treated at 1273 K. Accordingly, it is considered that the ductility of the HVOF coatings is appreciably higher compared to the HPS coatings.

The adhesion strength of the coatings was evaluated by the shear test using a specimen having a semicircular notch, as shown in Fig. 2. Figure 11 shows the measured shear adhesion strength of the coatings. The adhesion shear strength of the as-sprayed HVOF coating is about 300 MPa, which is about three times that of the HPS coating. The adhesion shear strength of the as-sprayed HVOF coating was about 200 MPa when measured with the test pieces having no semicircular notch.[10] The difference is caused by the stress concentration at the step of the test piece. Therefore, the adhesion shear strength using test pieces having no semicircular notch would be evaluated lower than that measurement in this work. On heat treatment at 1073 K for 3.6 ks, the adhesion strength of the HPS coating increased by about 1.5 times the as-sprayed coating. The adhesion strength of the HVOF coating also increased a little. This is caused by the diffusion between the coating and the substrate by heat treatment, as seen in Fig.7b and c. It is known that the coating of significantly high adhesion strength is obtained by HVOF process.

4. Summary

The properties of the Cr_3C_2 cermet coatings obtained by the HPS and HVOF processes were investigated by using SEM, EPMA, XRD, and the shear test.

The results obtained are summarized as follows.

- An amorphous phase forms in the as-sprayed HPS and HVOF coatings and decomposes on heat treatment up to 873 K.
- The hardness of the as-sprayed HVOF coating is higher than the hardness of the as-sprayed HPS coating. The hardness of the HPS coating increases appreciably with heat-treatment temperature due to the decomposition of the amorphous phase and the precipitation of Cr_3C_2 carbide.
- The ratio of the hardness measured with a large load to that measured with a small load can be used as an index to indicate the ductility of the coatings.

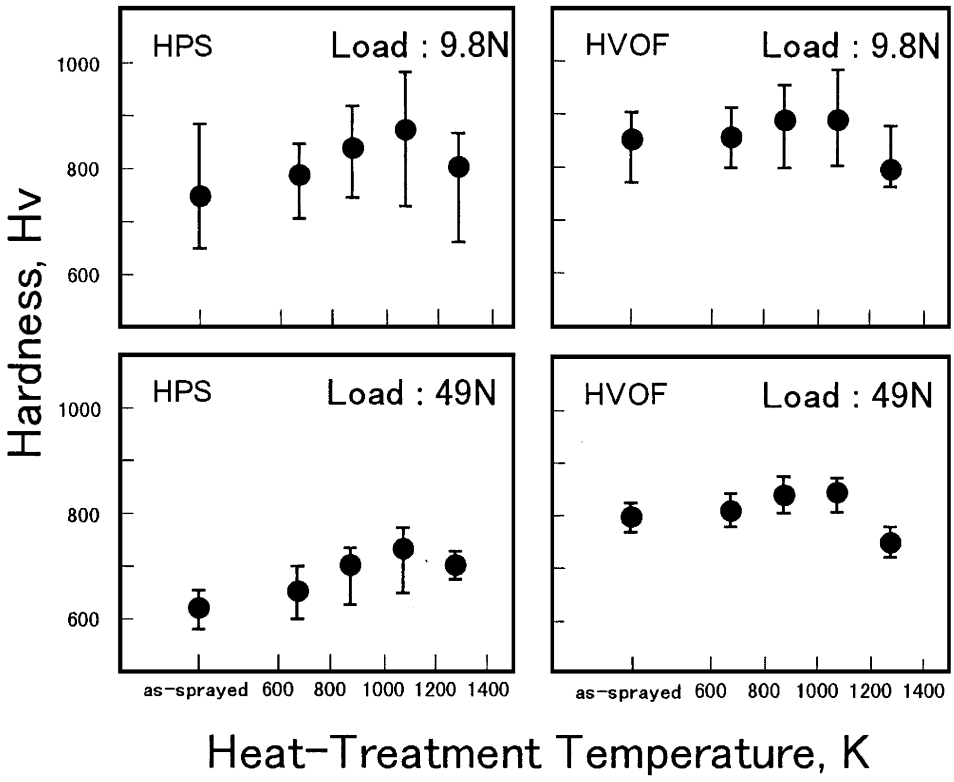

Fig. 8 Change in hardness as a function of heat-treatment temperature and load

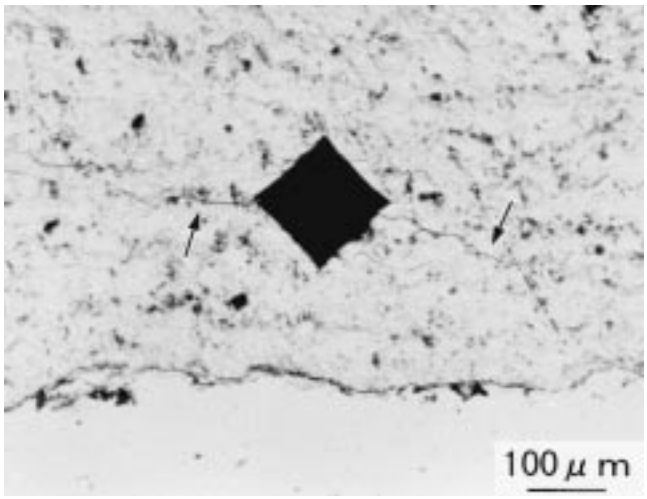

Fig. 9 Optical micrograph of as-sprayed coating. Indentation of as-sprayed HPS coating measured by a micro-Vickers hardness tester at a load of 49 N. Cracks are seen parallel to the sprayed layer

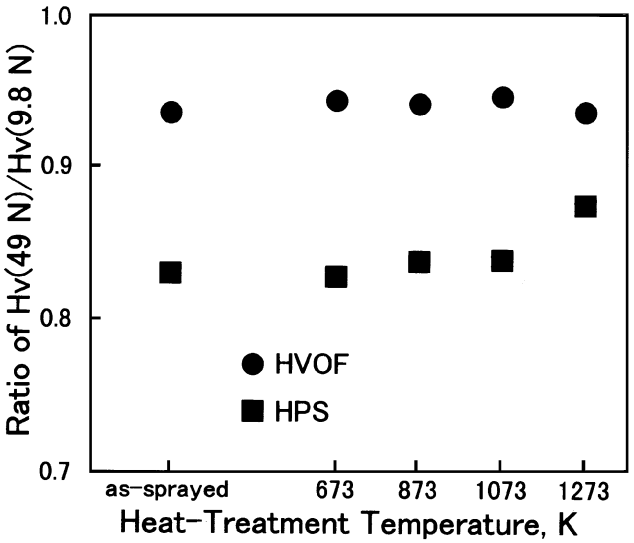

Fig. 10 Change in ratio of Hv (49N)/Hv (9.8 N) as a function of heat-treatment temperature

- The shear adhesion strength of the as-sprayed HVOF coating is 300 MPa, which is three times that of the adhesion strength of the HPS coating. The adhesion strength of the HPS coating increases by 1.5 times and that of the HVOF coating increases a little by heat treatment at 1073 K.

Acknowledgments

The authors acknowledge the Center for Instrumental Analysis, Kyushu Institute of Technology, for EPMA and XRD measurements, and Yamade Corrosion Protection of Metal Inc. for preparing the thermal-sprayed materials.

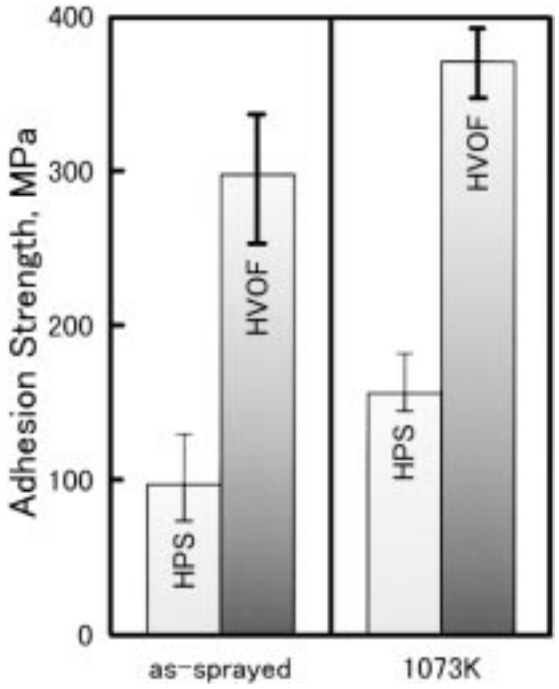

Fig. 11 Shear adhesion strength of coatings

References

1. K. Satoshi, S. Yuji, Y. Akihiro, I. Akira, and O. Hiromu: *Kawasaki Steel Giho*, 1987, vol. 19 (1), pp. 64-71 (in Japanese).
2. Chiyoshi Tonozaki: *Welding Technique*, 1988, vol. 36, pp. 75-84 (in Japanese).
3. Y. Fukuda, H. Yamasaki, M. Kumonn, and K. Kawamura: *Proc. Attac '88*, High Temperature Society of Japan, Osaka, Japan, 1988, pp. 49-54.
4. P. Chraska, J. Dubsky, B. Kolman, J. Ilavsky, and J. Forman: *J. Thermal Spray Technol.*, 1992, vol. 1 (4), pp. 301-06.
5. S. Rangaswarmy and H. Herman: *Advances in Thermal Spraying*, Pergamon Press, Elmsford, NY, 1986, pp. 101-10.
6. L. Russo and M. Dorfmann: in *Thermal Spraying—Current Status and Future Trends*, A. Ohmori, ed., High Temperature Society of Japan, Osaka, 1995, pp. 681-86.
7. S. Basinska-Pampuch and T. Gibas: *Ceram. Int.*, 1977, vol. 3 (4), pp. 152-58.
8. K.V. Rao, D.A. Somerville, and D.A. Lee: *Advances in Thermal Spraying*, Pergamon Press, Elmsford, NY, 1986, pp. 873-82.
9. E. Lugscheider, P. Remer, C. Herbst, K. Yushchenko, Y. Borisov, and A. Chernishov, P. Vitiaz, A. Verstak, B. Wielage, and S. Steinhäuser: in *Thermal Spraying—Current Status and Future Trends*, A. Ohmori, ed., High Temperature Society of Japan, Osaka, 1995, pp. 235-40.
10. H. Era, F. Otsubo, T. Uchida, S. Fukuda, and K. Kishitake: *Mater. Sci. Eng.*, 1998, vol. A251, pp. 166-72.
11. C.K. Lin, S.H. Leigh, and C.C. Berndt: in *Thermal Spraying—Current Status and Future Trends*, A. Ohmori, ed., High Temperature Society of Japan, Osaka, 1995, pp. 903-08.